

Detecting extra dimensions with gravity wave spectroscopy: the black string brane-world

Sanjeev S. Seahra, Chris Clarkson, Roy Maartens

Institute of Cosmology & Gravitation, University of Portsmouth, Portsmouth PO1 2EG, UK

(Dated: August 22, 2018)

Using the black string between two branes as a model of a brane-world black hole, we compute the gravity wave perturbations and identify the features arising from the additional polarizations of the graviton. The standard four-dimensional gravitational wave signal acquires late-time oscillations due to massive modes of the graviton. The Fourier transform of these oscillations shows a series of spikes associated with the masses of the Kaluza-Klein modes, providing in principle a spectroscopic signature of extra dimensions.

Black holes are central to our understanding of gravity, and are expected to be key sources of gravity waves that should be detected by the current and upcoming generation of experiments. Such a detection will not only confirm the indirect evidence from binary pulsars for gravity waves, but will also allow us to probe the properties of black holes and of gravity. In particular, this will open up a new window for testing modifications to general relativity, such as those arising from quantum gravity theories. String theory for example predicts that spacetime has extra spatial dimensions, so that the gravitational field propagates in higher dimensions and has extra polarizations. Recent developments in string theory indicate that Standard Model fields may be confined to a four-dimensional ‘brane’, while gravity propagates in the full ‘bulk’ spacetime. This has spurred the development of brane-world models, such as Randall-Sundrum (RS) type models, which can be used to explore astrophysical predictions [1]. RS type models have a five-dimensional bulk with negative cosmological constant, so that the metric is warped along the extra dimension. As a result, these models provide a new approach to the hierarchy problem, dimensional reduction and holography.

The nature of black holes that form by gravitational collapse on an RS brane is only partly understood [1, 2], and no exact solution is known for a black hole localized on one brane. If there is a second ‘shadow’ brane, the black string may be used to model large black holes on the visible brane, when the horizon on the brane is much greater than the extent of the horizon into the bulk [3]. The black string reproduces the Schwarzschild metric on the visible brane but is not confined to the brane, since there is a line singularity at $r = 0$ into the extra dimension (see Fig. 1). The shadow brane can also introduce an infra-red cut-off to shut down the Gregory-Laflamme (GL) instability of the black string at long wavelengths [4]. If the shadow brane is close enough to the visible brane for a given black hole mass M , or if M is large enough for a given brane separation d , then $GM e^{-d/\ell}/\ell$ is above a positive critical value and the GL instability is removed (see below). This is the background model that we perturb.

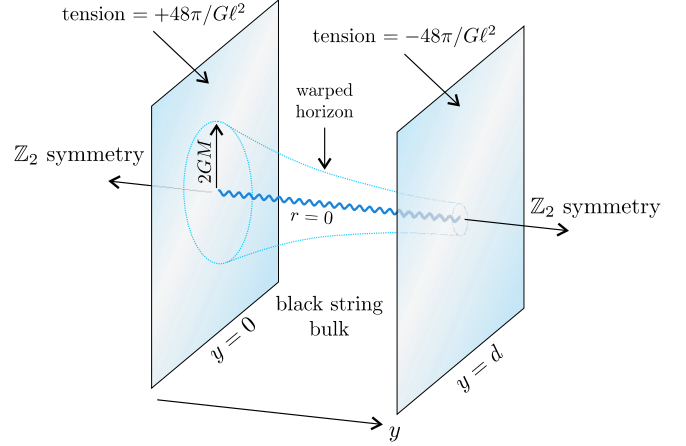


FIG. 1: Schematic of the black string

The brane separation is constrained from above by stability requirements. It is also constrained from below. This follows since the brane separation is a massless degree of freedom, felt on the visible brane as a ‘radion’ field, so that the low-energy effective theory on the visible brane is of Brans-Dicke type, with [5] $\omega_{\text{bd}} = 3(e^{2d/\ell} - 1)/2$, where ℓ is the bulk curvature radius. The shadow brane must be far enough away that its gravitational influence on the visible brane is within observational limits. Solar system observations impose the lower limit [6] $\omega_{\text{bd}} \gtrsim 4 \times 10^4$, so that $d/\ell \gtrsim 5$. The allowed region in parameter space is shown in Fig. 2. Table-top tests of Newton’s law impose the constraint $\ell \lesssim 0.1$ mm. This upper limit defines a mass $0.1 \text{ mm}/2G \sim 10^{-7} M_{\odot}$, so that for astrophysical black holes it follows that $2GM \gg \ell$ is easily satisfied: $GM/\ell \gtrsim 10^7 (M/M_{\odot})$.

The 5D black string is a solution of the Einstein equations $G_{AB} = 6\ell^{-2}g_{AB}$, with metric

$$ds^2 = a^2 (-f dt^2 + f^{-1} dr^2 + r^2 d\Omega^2) + dy^2, \quad (1)$$

where $f(r) = 1 - 2GM/r$, $a(y) = e^{-|y|/\ell}$, and the branes are at $y = 0, d$. Metric perturbations satisfy

$$\square h_{AB} + \nabla_A \nabla_B h^C_C - 2\nabla^C \nabla_{(A} h_{B)C} - 8\ell^{-2} h_{AB} = 0, \quad (2)$$

and gauge choices may be made to reduce the degrees

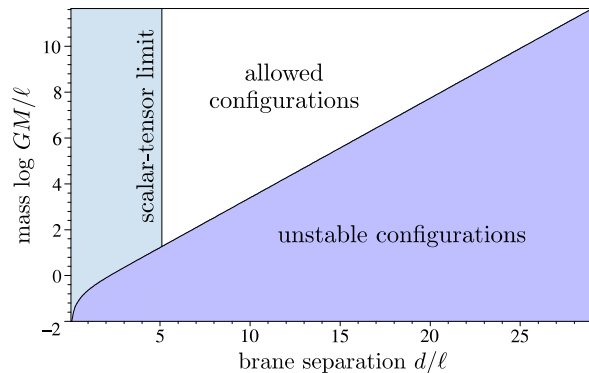


FIG. 2: The allowed region in parameter space. The stability boundary is well approximated by $GM/\ell = 0.1122e^{d/\ell}$.

of freedom to 5, the number of polarizations of the 5D graviton.

As in standard black hole perturbation theory [7], we use spherical harmonics Y_{lm} and their gradients to construct a basis $\mathbb{T}_{AB}^{(j,lm)}$ for h_{AB} , with $j = 1 \dots 15$. The metric perturbation is naturally split into two decoupled parts: polar [parity $(-1)^l$] and axial [parity $(-1)^{l+1}$]. Suppressing the (lm) indices, the expansion coefficients are of the form $\mathcal{C}^{(j)} = e^{i\omega\tau} H^{(j)}(r, y)$, where $\tau = t/GM$ and ω is a dimensionless frequency. We use two gauges, which are related by quadrature. We generalize the 4D Regge-Wheeler (RW) gauge by setting the coefficients of the most complicated harmonic tensors equal to zero, which makes the remaining coefficients gauge invariant. The RS gauge [5], given by $h^A_A = 0 = \nabla^B h_{AB} = h_{Ay}$, has the advantage that the expansion coefficients are separable: $\mathcal{C}^{(j)} = e^{i\omega\tau} W^{(j)}(r)Z(y)$, where [4]

$$a^2 Z'' - 2(aa')'Z = -m^2 Z. \quad (3)$$

Here, m is the effective mass on the visible brane of the Kaluza-Klein (KK) mode of the 5D graviton. The bulk wave functions $Z(y)$ are the same as those for Minkowski branes (even though the bulk is no longer anti de Sitter), and the solution for $m > 0$ is $Z(y) = B_2(m\ell/a)$, where B_2 is a linear combination of Bessel functions.

Neglecting brane bending, the boundary conditions at $y = 0, d$ in RS gauge are $\partial_y(a^{-2}h_{\alpha\beta}) = 0$. When $m = 0$, the solution is $Z \propto a^2$. For this zero-mode, the metric perturbations reduce to those of a 4D Schwarzschild metric, as expected. For $m \neq 0$, the boundary conditions lead to a discrete tower of KK mass eigenvalues,

$$m_n = (z_n/\ell)e^{-d/\ell}, \quad (4)$$

where $Y_1(m_n\ell)J_1(z_n) = J_1(m_n\ell)Y_1(z_n)$ [1]. The GL instability exists in the range $0 < m < m_{\text{crit}} \approx 0.4/GM$ [4]. If $m_1 > m_{\text{crit}}$, then the instability is avoided, and $m_1 = m_{\text{crit}}$ defines the stability curve in Fig. 2.

Radial master equations. We generalize the standard 4D analysis to find radial master equations for a reduced

set of variables, for all classes of perturbations. In the 5D case, the KK modes are governed by coupled master equations. These can be written as matrix-valued Schrödinger-like equations,

$$-\frac{d^2}{dx^2}\Psi + \mathbf{V}\Psi = \omega^2\Psi, \quad (5)$$

where \mathbf{V} is the potential matrix, $x = \rho + 2 \ln(\rho/2 - 1)$, and $\rho = r/GM$. For spherical (s-wave) polar perturbations, there is only one master variable, and

$$\frac{V_s}{f} = \frac{\mu^6 \rho^9 + 6\mu^4 \rho^7 - 18\mu^4 \rho^6 - 24\mu^2 \rho^4 + 36\mu^2 \rho^3 + 8}{\rho^3 (\mu^2 \rho^3 + 2)^2}, \quad (6)$$

where $\mu = GMm$. For $l \geq 2$ axial perturbations, there are two master variables and the potential matrix in the RW gauge is

$$\frac{\mathbf{V}_a}{f} = \mu^2 \mathbf{I} + \rho^{-3} \begin{bmatrix} l(l+1)\rho - 6 & \mu^2 \\ 4\rho^3 & l(l+1)\rho \end{bmatrix}. \quad (7)$$

The diagonal elements of \mathbf{V}_a are identical to the RW potentials for spin-2 and spin-1 excitations of 4D Schwarzschild, plus a mass term. Massive KK modes of the 5D graviton include spin-1 perturbations. (For $\mu = 0$, the spin-1 contribution is pure gauge.) For the other types of perturbations, we find that the $l = 1$ and $l \geq 2$ polar perturbations are governed by two and three master variables respectively, while there is only one master variable for the axial p-wave.

Stability. All master equations can be cast in the form $\mathcal{L}(\mu, \omega)\Psi = 0$, where \mathcal{L} is a linear differential operator. Stability holds if \mathcal{L} is positive definite when the boundary conditions $\Psi = 0$ are imposed at $x = \pm\infty$, and $\omega^2 < 0$ [7]. We have verified the positivity of \mathcal{L} analytically for all classes of axial perturbation. For the $l \geq 1$ polar case we performed a numerical search for solutions satisfying the above boundary conditions in the relevant region of (μ, ω) parameter space. No solutions were found, suggesting that no instability exists. The opposite is true for the s-wave case. The reason lies in the potential, which is shown in Fig. 3 for different values of μ . For small μ , there is a potential well that can support a normalizable bound state with $\omega^2 < 0$, which implies that \mathcal{L} is not positive definite. This well vanishes for large μ , suggesting that an instability exists for all modes with $0 < \mu < \mu_{\text{crit}}$. We used a standard WKB-inspired phase integral analysis [8] to develop a new improved derivation of the GL instability. Our approach leads to an accurate determination, $\mu_{\text{crit}} = 0.4301$, in agreement with recent results from full numerical relativity [9]. Stability is achieved if the mass of the first KK mode is such that $GMm_1 > \mu_{\text{crit}}$ (see Fig. 2).

Gravity wave signals. Perturbations of a stable black string describe gravitational radiation that may in principle be observable by current or future detectors. The

total gravity wave signal at the observer ($x = x_{\text{obs}}$) is a superposition of the waveforms $\psi_n(\tau)$ associated with the mass eigenvalues m_n of Eq. (3). In Fig. 4, we present signals associated with the four lowest masses for a marginally stable black string, for $l = 2$ axial modes. These are obtained by re-introducing time dependence into the Schrödinger equation (5), via $\omega \rightarrow -i\partial/\partial\tau$, and numerically integrating the resulting PDE with $\mathbf{V} = \mathbf{V}_a$. We assume static Gaussian initial data centered about $x = 50$ and an observer at $x_{\text{obs}} = 100$. Because the master equations reduce to the 4D RW equation when $\mu = 0$, the bottom curve exhibits the damped single-frequency (quasi-normal) ringing followed by a power-law tail familiar from the 4D analysis [7]. The massive mode signals are quite different [10], showing much less damping than the massless mode, and late-time monochromatic oscillations instead of a featureless power-law tail. This is reminiscent of the behaviour of massive scalar fields in 4D spherically symmetric spacetimes, where a detailed Green's function analysis shows [11] that the late-time signal is $\propto t^{-5/6} \sin mt$, irrespective of l .

To reconstruct the total waveform ψ_{tot} for the $l = 2$ axial case, as measured by an observer on the visible brane, we need to specify an initial profile F for the perturbation in the bulk. Using a conformal bulk coordinate $\xi = a^{-1}$, and assuming that F and Z_n are appropriately normalized, we have

$$\psi_{\text{tot}}(\tau) = \sum_n c_n Z_n(0) \psi_n(\tau), \quad c_n = \int_1^{e^{d/\ell}} \xi F Z_n d\xi, \quad (8)$$

where $\sum_n c_n^2 = 1$. Hence, c_n^2 is the fractional energy in the n -mode. Massive KK modes introduce striking new features in the gravity wave signal that are potentially observable, as shown in Fig. 5. The strength of the new features is sensitive to the initial data $F(\xi)$. Here we simply illustrate the possibilities via two forms of $F(\xi)$ that correspond to very different situations.

In Fig. 5, the upper signal has $d/\ell = 6$ [12], and the initial data $F(\xi)$ corresponds to the zero-mode $1/\xi^2$ with

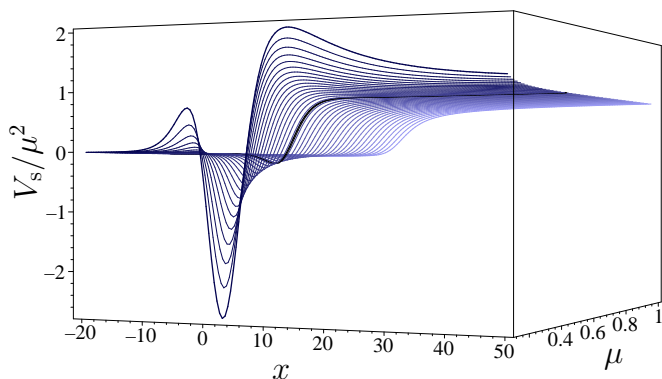


FIG. 3: The s-wave potential for varying μ . The critical potential is indicated by the heavy line. For $\mu < \mu_{\text{crit}}$, there is a bound state with $\omega^2 < 0$, indicating an instability.

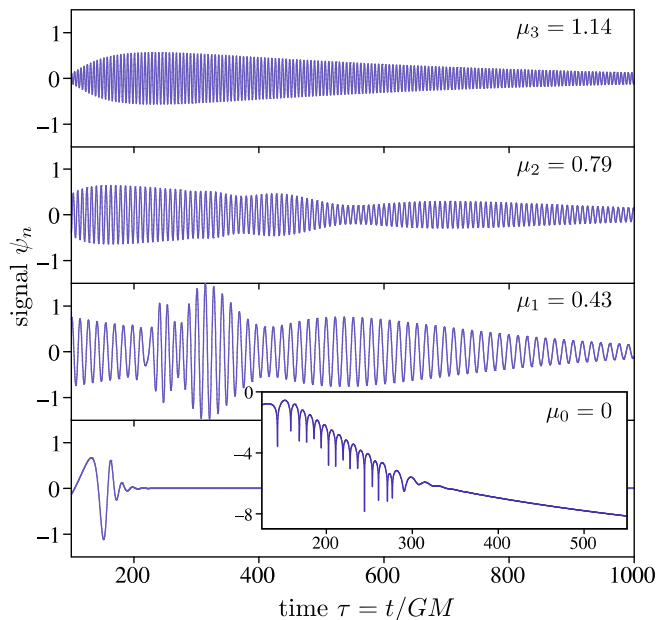


FIG. 4: Gravity wave signals associated with 3 massive KK modes and the 0-mode of $l = 2$ axial perturbations, for a marginally stable black string. The inset shows the zero-mode signal on a logarithmic scale.

a cut-off applied one eighth of the distance to the shadow brane. This data is motivated by the results of numerical calculations of the bulk gravitational field around a small brane-localized black hole [2]. If the black hole mass is small enough to be in the unstable region of Fig. 2, we may think of the black hole as the endpoint of a GL instability [2, 9]. The initial data is then thought of as arising from an encounter between this black hole and the much heavier black string. We find that in this case, the coefficients of the massive mode signals are of order 10^{-4} , which suggests that the total waveform will only exhibit minor deviations from the GR prediction. This is certainly true for early times, where the signal is dominated by ordinary 4D Schwarzschild quasi-normal ringing (*cf.* the inset of Fig. 4). However, as can be inferred from the individual massive waveforms in Fig. 4, the late-time signal is very different from the 4D case—it is both oscillatory and very lightly damped. The inset shows the Fourier transform of the signal for late times. There are eight discrete peaks in the spectrum, corresponding to each of the eight non-zero mass modes.

In the lower panel, we take $d/\ell = 20$ and Gaussian initial data in the bulk centered halfway between the branes (if the center is moved closer to the shadow brane, the results are qualitatively similar). This could correspond to an event which ‘mainly takes place in the bulk’, such as the merger of two black strings. In this case, the zero mode waveform is dominated by the massive mode signals, and the waveform is very different from the 4D case. The contributions from the odd modes m_3 , m_5 and m_7 are suppressed, which results in a late-time transform

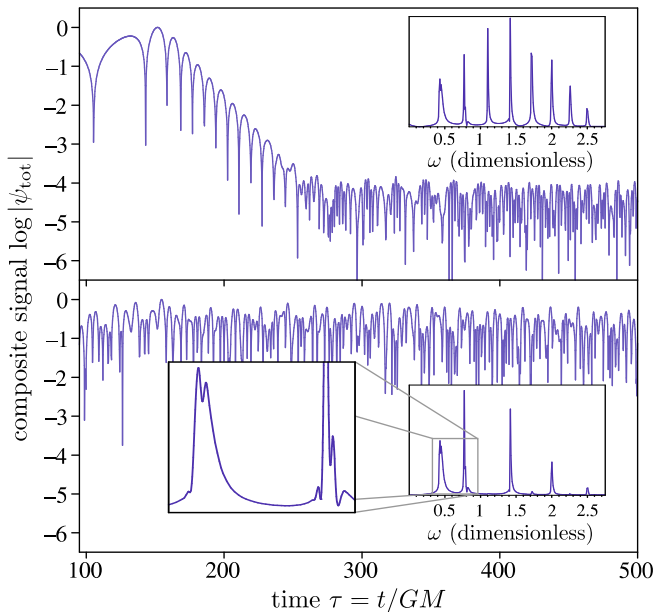


FIG. 5: Composite $l = 2$ axial gravity wave signal (normalized) from the 9 lowest mass modes of a marginally stable black string. The upper panel corresponds to ‘truncated zero-mode’ bulk initial data with $d/\ell = 6$, the lower panel to Gaussian bulk initial data with $d/\ell = 20$. Insets show the Fourier transform of the respective waveforms for $300 \leq \tau \leq 1000$. The percentage of energy in the 4D zero-mode part of the signal is 99.96 % (upper) and 2.281×10^{-13} % (lower).

with five principal peaks in the inset. These peaks in fact display a degree of fine structure, as shown in the blow-up, that deserves further investigation.

Conclusions. Will the consideration of other types of perturbations or different multipoles in some way contaminate the spectroscopic signal? We find that in all cases, as $r \rightarrow \infty$, master variables with $\mu \neq 0$ behave as massive fields propagating on Schwarzschild spacetime, which is enough to guarantee the slowly-decaying oscillating tail. Massless modes for $l > 2$ are known to be subject to more damping than for $l = 2$, so if the massive signal dominates the latter for late times, it will also dominate the former.

Can the massive signal be resolved by realistic gravity wave detectors? There are two separate issues: the frequency of the massive modes and their relative amplitude. From the formulas above, one finds that the discrete frequencies in the late-time tail are

$$f_n = z_n e^{26.9-d/\ell} (0.1 \text{ mm}/\ell) \text{ Hz}. \quad (9)$$

For $d/\ell \gtrsim 5$, z_n is well approximated by $J_1(z_n) = 0$. Note that unlike 4D black hole quasinormal modes, these frequencies are *independent* of the mass M . Taking $\ell = 0.1 \text{ mm}$ and $d/\ell = 24$, results in $f_1 \sim 100 \text{ Hz}$, which is ideal for a LIGO detection of extra dimensions. For $d/\ell = 33$, we find an optimal LISA signal, with $f_1 \sim 0.01 \text{ Hz}$. For these parameters, the lower limits on black string masses are $M > 100 M_\odot$ and $M > 10^6 M_\odot$, respectively.

In regard to the amplitudes, the most optimistic type of events involve bulk-based initial data, i.e., black string mergers. Since the zero-mode energy is small in these situations, we expect the strength of the massive mode oscillations to be comparable to the quasinormal ringing amplitude in the analogous 4D case. The situation is more delicate for brane based initial data, where the zero mode-tends to dominate the signal. We find that the relative massive amplitude tends to increase with decreasing d/ℓ . However, small d/ℓ implies large f_n , so the best prospect of seeing this type of signal lies with high frequency detectors.

The discrete nature of the late-time Fourier transform of the black string waveform is the most important observable feature of this model. Its detection would provide clear evidence of extra dimensions. It would also give the direct spectroscopic measurement of the KK masses m_n , which in turn provides information about d and ℓ . Although we have analyzed a specific model of brane-world black holes, we expect that qualitatively similar features will arise for other models with compact extra dimensions, since they all have a discrete tower of massive KK modes. Furthermore, since the massive modes travel below light-speed, there will be potentially observable time-delay in their arrival, which could be of order seconds or longer for distant sources. Also, the light damping of KK modes means that they may have a significant integrated contribution to the stochastic gravity wave background.

Acknowledgements SSS is supported by NSERC, CC and RM by PPARC. We thank C Kiefer, B Kol, K Koyama, D Langlois and J Soda for discussions.

-
- [1] See e.g., R. Maartens, Liv. Rev. Rel. **7**, 1 (2004).
 - [2] H. Kudoh, T. Tanaka, and T. Nakamura, Phys. Rev. D**68**, 024035 (2003).
 - [3] S. Kanno, and J. Soda, Class. Quant. Grav. **21**, 1915 (2004).
 - [4] R. Gregory, Class. Quant. Grav. **17**, L125 (2000).
 - [5] J. Garriga and T. Tanaka, Phys. Rev. Lett. **84**, 2778 (2000).
 - [6] B. Bertotti, L. Iess, and P. Tortora, Nature **425**, 374 (2003); C. M. Will and N. Yunes, gr-qc/0403100.
 - [7] See, e.g., H. Nollert, Class. Quant. Grav. **16**, R159 (1999).
 - [8] N. Froeman, P. O. Froeman, N. Andersson, and A. Hoekback, Phys. Rev. D**45**, 2609 (1992).
 - [9] M. W. Choptuik, et al., Phys. Rev. D**68**, 044001 (2003).
 - [10] Amplitude modulations in the massive mode signals are also found in the case of Minkowski branes: A. O. Barvinsky, A. Y. Kamenshchik, A. Rathke, and C. Kiefer, Annalen Phys. **12**, 343 (2003).
 - [11] H. Koyama and A. Tomimatsu, Phys. Rev. D**65**, 084031 (2002).
 - [12] For numerical convenience we choose the marginally stable case, so that $M \ll M_\odot$ for $d/\ell = 6$, but the results will be qualitatively similar for $M \gtrsim M_\odot$.